Sizeable beta-strength in ^{31}Ar (β3p) decay

G.T. Koldste [a], B. Blank [b], M.J.G. Borge [c], J.A. Briz [c], M. Carmona-Gallardo [c], L.M. Fraile [d], H.O.U. Fynbo [a,*], J. Giovinazzo [b], J.G. Johansen [a,1], A. Jokinen [e], B. Jonson [f], T. Kurturkian-Nieto [b], T. Nilsson [f], A. Perea [c], V. Pesudo [c], E. Picado [c,g], K. Riisager [a], A. Saastamoinen [e,2], O. Tengblad [c], J.-C. Thomas [h], J. Van de Walle [i]

[a] Department of Physics and Astronomy, Aarhus University, DK-8000 Aarhus C, Denmark
[b] Centre d'Études Nucléaire de Bordeaux-Gradignan, CNRS/IN2P3 – Université Bordeaux I, F-33175 Gradignan Cedex, France
[c] Instituto de Estructura de la Materia, CSIC, E-28006 Madrid, Spain
[d] Grupo de Física Nuclear, Universidad Complutense, CEI Moncloa, E-28040 Madrid, Spain
[e] Department of Physics, University of Jyväskylä, FIN-40351 Jyväskylä, Finland
[f] Fundamental Fysik, Chalmers Tekniska Högskola, S-41296 Göteborg, Sweden
[g] Sección de Radiaciones, Universidad Nacional, Heredia, Costa Rica
[h] GANIL, CEA/DSM–CNRS/IN2P3, F-14076 Caen Cedex 5, France
[i] CERN, CH-1211 Geneva 23, Switzerland

ABSTRACT

We present for the first time precise spectroscopic information on the recently discovered decay mode β-delayed 3p-emission. The detection of the 3p events gives an increased sensitivity to the high energy part of the Gamow–Teller strength distribution from the decay of ^{31}Ar revealing that as much as 30% of the strength resides in the β3p-decay mode. A simplified description of how the main decay modes evolve as the excitation energy increases in ^{31}Cl is provided.

© 2014 The Authors. Published by Elsevier B.V. This is an open access article under the CC BY license (http://creativecommons.org/licenses/by/3.0/). Funded by SCOAP^3.

1. Introduction

When the dripline is approached, the energy window for β-decays increases so that delayed nucleon emission eventually becomes possible. The most intensely studied decay mode is β-delayed proton emission, since protons are easy to detect and the dripline lies closer to stability for proton-rich nuclei. For a review of β-delayed particle emission see Ref. [1–3]. ^{31}Ar is one of the most studied β-delayed proton emitters on the dripline. During the past three decades work on ^{31}Ar has focussed on the physics of β-delayed one- and two-proton emission; here we demonstrate how the decay of ^{31}Ar can also be used to gain insight into the contribution of β-delayed three-proton emission to exotic decays at the dripline.

The β3p-decay mode was only recently discovered in the decay of ^{31}Ar [4] and it has previously only been observed in two other cases: ^{45}Fe [5] and ^{43}Cr [6,7]. The information on the decay mode from these experiments is limited to the identification of its existence, since they all used Time Projection Chambers in which the energy resolution is low for four body decays.

With a compact setup for particle detection consisting of six double sided Si strip detectors, we have for the first time obtained precise energy and angular information on a sample of β-delayed 3p-decays. This enables both a quantitatively and qualitatively new understanding of the decay mode including a significantly improved determination of the high energy part of the Gamow–Teller strength distribution in the decay of ^{31}Ar.

In most previous studies of decays with open β2p-emission channels, decays to the Isobaric Analogue State (IAS) have been dominant. Most of the early analysis of decay mechanisms focussed on this, for example the theoretical treatment of β2p-emission by Détraz [8]. We now know that this picture is incomplete, since previous ^{31}Ar experiments have shown that many other levels in the β-daughter also can contribute significantly to the delayed 2p-emission. Hence, we need to expand conceptually upon the picture used by Détraz and allow for more states to be populated in the β-daughter. Proton emitting levels close to a threshold tend to give distinct lines, whereas levels at higher

excitation energy decay into so many channels that a statistical approach may become more appropriate. The same effect makes βp-spectra significantly smoother at high Z, see e.g. Ref. [3]. We shall here consider a simplified model, with the aim of focussing on the conceptual issues rather than providing a detailed description of the decay.

It was realised early [9,10] for nuclei close to stability that one-neutron emission, two-neutron emission, etc., decay modes follow each other as dominating decay modes as the excitation energy in a nucleus is increased. It is thus natural to investigate if a similar sequence appears for β-delayed proton emission. Here the ^{31}Ar decay constitutes an ideal case because it has a sizeable Q-value for three-proton emission, while e.g. the neutron channel only opens above the Q_{EC}-window of 18.38(10) MeV [11].

In this letter we first describe our experimental data and give an overview of what information the detailed 3p-spectroscopy can provide. We then focus on the Gamow–Teller distribution and the evolution of decay modes as excitation energy increases.

2. Three-proton detection

The experiment was performed at ISOLDE, CERN using a 60 keV beam of ^{31}Ar. The beam was collected in a 50 μg/cm^2 carbon foil situated in the center of six double sided silicon strip detectors (DSSSD) (the detector thicknesses were 69 μm, 494 μm, and four with thicknesses around 300 μm). Most of the DSSSDs were backed by thick unsegmented Si detectors. Outside the chamber two Miniball germanium cluster detectors were situated for detection of γ-rays [12]. A detailed description of the setup including detector placements, calibration and cuts used in the data analysis can be found in Refs. [11,13]. β-particles deposit of the order of 300 eV/μm in silicon while the energy of most protons is in the MeV range, and so the discrimination between protons and β-particles is mainly based on the deposited energy in the detector. Unless otherwise stated we use a low energy cut-off of 800 keV for the protons, but allow the lowest energy proton in multi-proton events to have as little as 500 keV unless it is detected by the thick strip detector, where the β-particles can deposit somewhat higher energy than that.

Ref. [11] contains a detailed analysis of the Fermi strength of the decay of ^{31}Ar and the different decay modes of the IAS. This includes the contribution from the 3p-decay of the IAS, which is clearly identified in the Q_{3p}-spectrum extracted from the multiplicity-three events shown in Fig. 1. Included is also (purple (grey) dashed line) a simulation of the 3p-decay from the IAS to the ground state of ^{28}Si (downscaled) to show the energy resolution of the 3p-detection. The full width at half maximum (FWHM) for 3p-decays found from simulations is approximately 0.3 MeV, mainly due to the reconstruction of the energy of the recoiling ^{28}Si nucleus. The resolution for detection of individual protons is 0.05 MeV FWHM. It is clearly seen in Fig. 1 that only about half of the events stem from decays of the IAS. The rest is interpreted as coming from levels with excitation energies mainly above the IAS. This implies that there is a contribution to the Gamow–Teller strength which needs to be extracted by a detailed analysis of the β3p-events. This enables for the first time the inclusion of this decay mode in the determination of the Gamow–Teller distribution, which is done in Section 3.

3. The Gamow–Teller distribution

The extraction of the Gamow–Teller strength is much more complicated than the extraction of the Fermi strength, since one has to include all decay modes of the many levels populated in
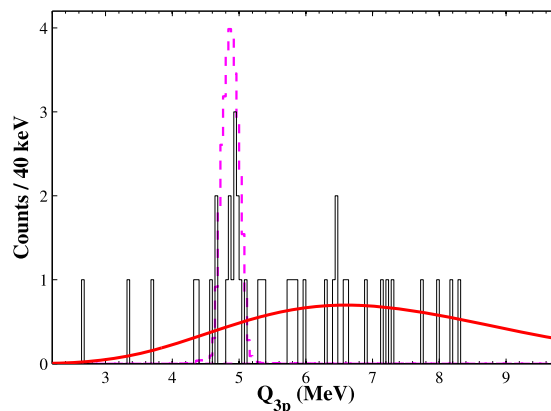

Fig. 1. (Colour online.) Q_{3p} calculated for multiplicity-three events. The dashed line is a simulation of a 3p-decay of the IAS in ^{31}Cl to the ground state in ^{28}Si. The full curve is the χ^2-distribution function (see text) from Fig. 5 folded with itself three times and scaled manually to fit the data.
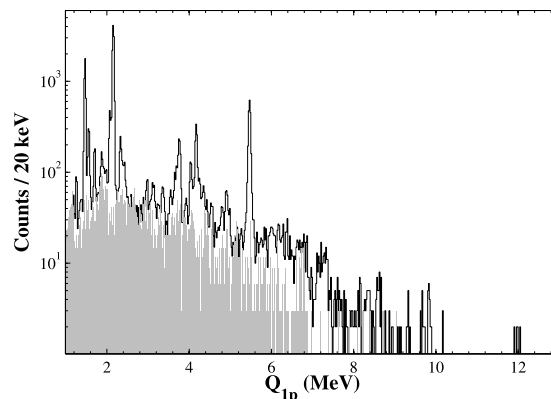

Fig. 2. The Q_{1p}-spectrum calculated for all the particles that have hit the best performing detector in the setup. Also shown is the normalised background from two-proton events estimated from coincidence data (grey).

^{31}Cl. It has been attempted previously in an experiment similar to this by Fynbo et al. [14]. In the present experiment the energy and angular resolutions are significantly improved and we can now for the first time include the 3p-component. The Gamow–Teller strength is defined as (excluding the IAS):

$$B_{GT} = \left(\frac{g_A}{g_V}\right)^{-2} \frac{C \cdot b}{f \cdot T_{1/2}},$$

where $C = 6144.2(16)$ s and $g_A/g_V = -1.2694(28)$ [15], the f-value can be found using Ref. [16], the total half-life, $T_{1/2} = 15.1(3)$ ms, determined using these data [11] and the branching ratio, b, can be deduced from the data using the Q_{1p}-, Q_{2p}- and Q_{3p}-spectra.

To make a precise determination of the branching ratio, it is important not only to have a good energy resolution, but also to precisely know the detection efficiency and the total number of collected ^{31}Ar isotopes. For this reason only the two best performing of the six detectors are singled out for analysis of the Q_{2p}-spectrum, while for the Q_{1p}-spectrum only the best performing detector is used. This choice is caused by larger uncertainties in the energy calibration for high energies for the other detectors. Since the number of 3p-events is so limited, all detectors are included in the Q_{3p}-spectrum.

The Q_{1p}-spectrum is shown in Fig. 2. A lower cut-off of 1 MeV is used since the spectrum below is dominated by background. There is a contribution from 2p-decays to the multiplicity-one pro-
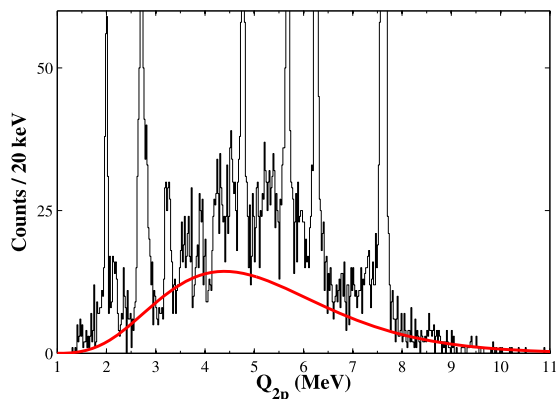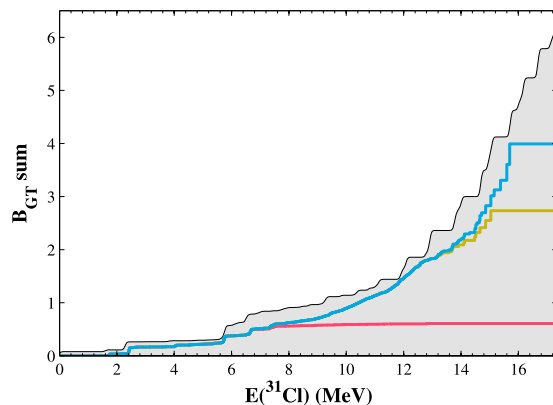
Fig. 3. (Colour online.) Q_{2p} calculated for multiplicity-two events. The vertical range has been cut off for better visualisation of the unresolved structure. The red/grey curve is the χ^2-distribution from Fig. 5 folded with itself and manually scaled to the data.


Fig. 4. (Colour online.) The total summed Gamow–Teller strength from 1p-, 2p- and 3p-events (blue upper curve) as a function of excitation energy in ^{31}Cl in the full Q_β-energy window (17.36(10) MeV). Also shown are the summed B_{GT}-spectrum from the 1p-events (pink lower curve) and for both the 1p- and 2p-events (yellow middle curve). The shaded area shows the summed Gamow–Teller strength from a shell-model calculation in the full sd-shell [14].

ton spectrum, which must be subtracted when the B_{GT} distribution from events leading to bound states in ^{30}S is estimated. There are also a number of peaks known to stem from decays of the IAS, which are also removed. Finally some transitions are known not to feed the ground state of ^{30}S. The peaks known to go to excited levels in ^{30}S below 5.2 MeV (listed in Table 2 of Ref. [14]) are shifted upwards with the excitation energy of 2210.2 keV, 3404.1 keV, 3673 keV and 5136 keV. Notice that an average energy (3673 keV) for the third (0^+) and fourth (1^+) level is used, since their energies are so close to each other that it is not possible to deduce which one is populated. The branching ratio is then evaluated bin by bin and the B_{GT} strength deduced.

For the Q_{2p}-spectrum shown in Fig. 3 a low-energy cut-off of 500 keV is used for both protons (the spectrum can be seen in Ref. [11, Fig. 8]). In Fig. 3, only the three peaks located at 7.6 MeV, 6.3 MeV and 5.7 MeV correspond to decays from the IAS. For the extraction of the B_{GT} strength they are removed by setting the B_{GT}-value in these bins to be the average of the values in the bins on each side of the peaks. Some of the remaining 2p-decays will also correspond to transitions to excited states in ^{29}P, but at the current level of statistics we cannot identify those transitions and they are therefore all assumed to feed the ground state in ^{29}P. This assumption means that we systematically shift some of the B_{GT} strength to lower energy and somewhat underestimate the total B_{GT} strength.

Finally, the 3p-data used are shown in Fig. 1. Here the decays from the IAS are the events between 4.3 MeV and 5.5 MeV. Thus only events above 5.5 MeV are used for the extraction of the B_{GT} strength. Again all events are assumed to go to the ground state of ^{28}Si.

The total summed B_{GT}-spectrum obtained from the three spectra can be seen in Fig. 4 (blue upper curve). The individual contributions from the 1p-events (pink lower curve) and for the sum of the 1p- and 2p-events (yellow middle curve) are also shown. The total observed Gamow–Teller strength in the 1p-spectrum is 0.61(3)(7) compared to 0.58(3) found in Ref. [14]. The uncertainty is composed of two contributions, where the first is comprised of (in order of importance) counting statistics, the Q-value, the half-life, and setup related uncertainties, while the latter is the 11% uncertainty on the absolute branching ratio of the main 1p-peak [17] used to extract the number of ^{31}Ar ions in the experiment. This uncertainty was not correctly included in Ref. [14]. In the 2p-spectrum the total observed Gamow–Teller strength is 2.1(3)(2) compared to 1.86(12) in Ref. [14] and in the 3p-spectrum it is 1.26(15)(14). As already mentioned, there is a systematic bias for the extracted strength to underestimate the true strength because

all transitions are assumed to populate the ground state in the 1p, 2p or 3p daughters unless population of excited states is explicitly measured from coincident gamma rays. In Fig. 4 the total observed Gamow–Teller strength is compared with a shell-model calculation in the full sd-shell model space ($0d_{5/2}$, $1s_{1/2}$ and $0d_{3/2}$) using the Wildenthal universal 11 (USD) effective interaction [18] and a quenching factor of 0.77, see [14] for further details. The experimental and theoretical curves follow each other closely, indicating that most of the Gamow–Teller strength has been measured up to about 15.7 MeV. At the highest energies there is more strength predicted than experimentally identified, however, the missing strength corresponds to only 1–2 events missing in that energy region, which means that the deviation between data and theory is not statistically significant.

The one-proton decay mode contributes up to 12.85 MeV and the two-proton decay mode starts contributing at 5.90 MeV, but it can be seen that from around 7.5 MeV the contribution from the two-proton decay mode dominates. The two-proton decay mode contributes until 15.04 MeV and the three-proton decay mode is observed for the Gamow–Teller beta decay at 13.16 MeV and dominate above 15.04 MeV. From this it is already seen that there is an evolution in the dominating decay modes, i.e. more protons are emitted with increasing excitation energy, as is known to be the case for neutron emission from nuclei close to stability [9,10]. This behaviour is investigated in more detail in the following section.

4. Evolution of decay modes

The energy distribution of the emitted protons from a given level depends on three factors: The phase-space, which grows proportional to the proton energy, the level density in the daughter nucleus, which increases with excitation energy, and the penetrability of the proton, which decreases strongly with decreasing energy [19]. At low proton energy the spectrum is dominated by the penetrability and we expect decay branches to be suppressed if the penetrability is less than 10^{-3}. Since ^{31}Ar has spin $\frac{5}{2}^+$, we only populate $\frac{3}{2}^+$, $\frac{5}{2}^+$ and $\frac{7}{2}^+$ levels in ^{31}Cl and given the structure of ^{31}Ar we expect the emitted protons to be predominantly from the sd-shell, and hence $l = 0, 2$ to be favoured in the proton emissions. The penetrability of 10^{-3} corresponds to proton energies of around 0.8 MeV for s-wave transitions and around 1.3 MeV for d-wave transitions for the isotopes involved in the decay and
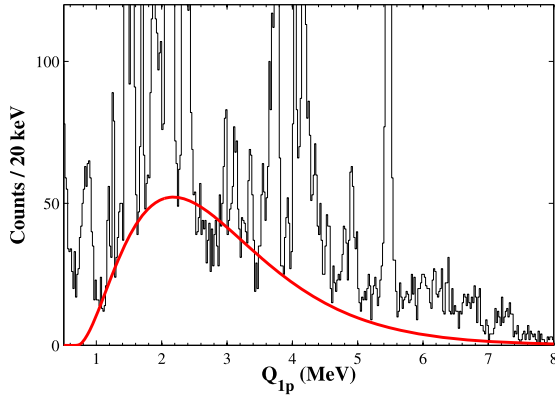
Fig. 5. (Colour online.) Q_{1p} calculated for all particles detected in detector 3. The vertical range has been cut off for better visualisation of the unresolved structure. The red/grey curve is the χ^2-distribution from Fig. 6 transformed using the recoil factor and scaled manually to fit the data.

Fig. 6. (Colour online.) Energies of the individual protons detected in multiplicity-two events. The vertical range has been cut off for better visualisation of the unresolved structure. The red/grey curve is a χ^2-distribution adjusted to the data manually: $h_{2p} = 610 \cdot \chi^2(2.8 \cdot \frac{E}{\text{MeV}} - 2.0)$.

we thus expect decay branches with proton energies below this to be suppressed. For high energies the level density will be so high that the decay can be treated purely statistically [3]. In Ref. [8] the intensity of protons as a function of energy is calculated and plotted for the decay of the IAS taking into account all three factors. The result is a bell-shaped curve, with a long upper tail. Expanding this to the case here, where multiple levels in ^{31}Cl are populated, the energy distribution should be a sum of similar curves, shifted slightly in energy. The result is likely to be a curve of similar shape. This will also be the case for decays of excited levels in both ^{29}P and ^{30}S, and thus also when one considers the two- and three-proton energy spectra. However, for levels close to the threshold this way of thinking breaks down, and the decay will instead give a number of resolved lines in the spectrum. We now check our current sensitivity to modelling via a crude model with only little physics input: first, that the three stages of proton emission are independent, and second that they can each be described by the same distribution.

We now explore whether our data, apart from the resolved lines, can be described by assuming all emitted protons to stem from the same distribution.
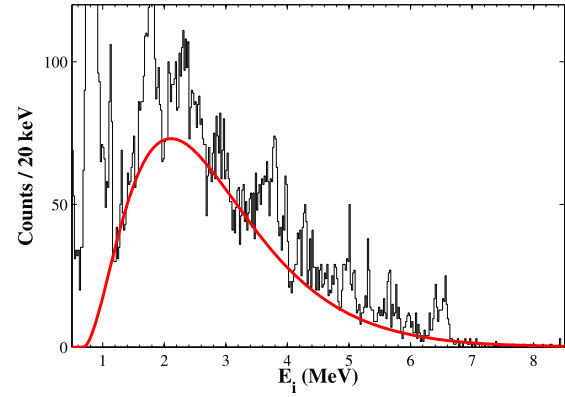
We first consider the energy spectrum for two-proton events in Fig. 6. The reason for starting with the two-proton spectrum is that the levels fed in ^{30}S have a sufficiently large excitation energy so that the level density is high. Therefore this spectrum contains fewer resolved lines than the one-proton spectrum. The major resolved lines around 0.7 MeV are most likely due to an overlap in the structure of ^{31}Ar and the 5.2 MeV state fed in ^{30}S. Disregarding the resolved lines in the spectrum the energy distribution does seem to have the same shape as calculated by Détraz in Ref. [8], i.e. a bell-shape with a long upper tail. A well known function with this shape is the χ^2-distribution. By manually adjusting the parameters of this function to the data the following function results

$$h_{2p} = 610 \cdot \frac{1}{2^{\frac{6}{2}}\Gamma(\frac{6}{2})} x^{\frac{6}{2}-1} e^{-\frac{x}{2}},$$
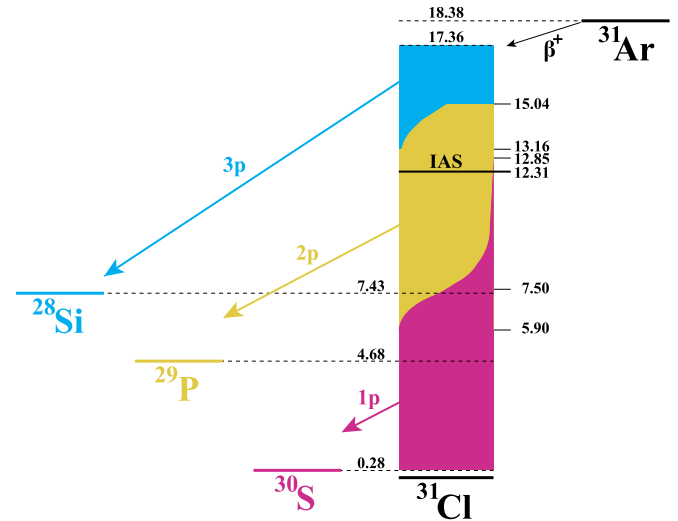
$$x = 2.8 \cdot \frac{E}{\text{MeV}} - 2.0,$$

which is shown together with the data in Fig. 6. The distribution has an average energy of 2.86 MeV.

Multiplying the energy with the recoil factor one gets the typical value of Q_{1p}. This is scaled and plotted in Fig. 5 together with the Q_{1p}-value for all particles which hit detector 3 (the same de-

tector as used in Section 3). Again disregarding the resolved lines, the shape of the data seem to fit the distribution.

By folding the distribution with itself the typical value of Q_{2p} is obtained corresponding to randomly adding the energies of the two protons. The Q_{2p}-spectrum can be seen in Fig. 3 together with this distribution, which is again scaled to fit the data. Also here the simple model describes the data fairly well, when disregarding the resolved lines.

Finally folding the distribution with itself once more gives the typical values of Q_{3p}. This is shown in Fig. 1 together with the data. Here the statistics is very limited, but the data is consistent with the trend displayed by the simple model.

A schematic view of the decay mode as a function of excitation energy in ^{31}Cl is shown in Fig. 7. The approximate percentage of the decay occurring by the three decay modes is shown by colour to illustrate how they evolve as a function of excitation energy. Here it is clearly seen how the 1p-decay dominates for the low-lying levels in ^{31}Cl. When the excitation energy increases the 2p-decay takes over and finally the 3p-decay dominates for the very high excitation energies. As mentioned this is the same trend as is seen previously for neutron emission.

Fig. 7. (Colour online.) A schematic view of the decay of ^{31}Ar. The pink (dark grey), yellow (light grey) and blue (medium grey) correspond to 1p-, 2p- and 3p-decays respectively and are approximately pictured with the percentage of the proton decay as a function of excitation energy in ^{31}Cl.

It should be stressed that the fitted curves are only simplified models and that they are not fitted to the data, but only adjusted and scaled manually. However, it is remarkable that with this very simple approach it is possible to relate Q_{ip}-distributions (for $i = 1, 2, 3$) to each other. This relation may be exploited for other proton-rich isotopes to estimate energy scales involved in $\beta 3p$-decays from observed 1p- and 2p-spectra and thereby judge if this decay mode could be relevant.

5. Summary

Using the precise energy information on the β-delayed 3p-decay of ^{31}Ar, which is obtained for the first time, we have significantly improved the determination of the high energy part of the Gamow–Teller strength distribution. The identified summed B_{GT} from the 3p-decay is found to be 1.26(15)(14), which is of the order of 30% of the observed strength. By comparison with a shell-model calculation we have shown that we, using our 1p-, 2p- and 3p-data, can account for the majority of the expected strength distribution.

We have shown that one-proton emission, two-proton emission and three-proton emission decay modes follow each other as dominating decay modes as the excitation energy in a nucleus is increased, as is the case for nuclei close to stability. Furthermore, we have shown that with a simplified model it is possible to give an estimate of the Q_{2p}- and Q_{3p}-distributions from the Q_{1p}-distribution, when disregarding resolved lines.

Acknowledgements

References

[1] B. Blank, M. Borge, Nuclear structure at the proton drip line: advances with nuclear decay studies, Prog. Part. Nucl. Phys. 60 (2008) 403, http://dx.doi.org/10.1016/j.ppnp.2007.12.001.

[2] M. Pfützner, et al., Radioactive decays at limits of nuclear stability, Rev. Mod. Phys. 84 (2012) 567, http://dx.doi.org/10.1103/RevModPhys.84.567.

[3] M.J.G. Borge, Beta-delayed particle emission, Phys. Scr. 2013 (T152) (2013) 014013.

[4] M. Pfützner, et al., Observation of beta-delayed three-proton emission from ^{31}Ar with the optical time projection chamber at the FRS, GSI Sci. Rep. (2012) 147.

[5] K. Miernik, et al., First observation of β-delayed three-proton emission in ^{45}Fe, Phys. Rev. C 76 (2007) 041304, http://dx.doi.org/10.1103/PhysRevC.76.041304.

[6] M. Pomorski, et al., β-delayed proton emission branches in ^{43}Cr, Phys. Rev. C 83 (2011) 014306, http://dx.doi.org/10.1103/PhysRevC.83.014306.

[7] L. Audirac, et al., Direct and β-delayed multi-proton emission from atomic nuclei with a time projection chamber: the cases of ^{43}Cr, ^{45}Fe, and ^{51}Ni, Eur. Phys. J. A 48 (2012) 179, http://dx.doi.org/10.1140/epja/i2012-12179-1.

[8] C. Détraz, The branching ratio of β-delayed two-proton emission, Z. Phys. A 340 (1991) 227, http://dx.doi.org/10.1007/BF01294668.

[9] S.N. Ghoshal, An experimental verification of the theory of compound nucleus, Phys. Rev. 80 (1950) 939, http://dx.doi.org/10.1103/PhysRev.80.939.

[10] P. Morrison, A survey of nuclear reactions, in: E. Segre (Ed.), Part VI of Experimental Nuclear Physics, vol. II, John Wiley, 1953.

[11] G.T. Koldste, et al., Multi-particle emission in the decay of ^{31}Ar, Phys. Rev. C 89 (2014) 064315, http://dx.doi.org/10.1103/PhysRevC.89.064315, http://link.aps.org/doi/10.1103/PhysRevC.89.064315.

[12] N. Warr, et al., The Miniball spectrometer, Eur. Phys. J. A 49 (2013) 40, http://dx.doi.org/10.1140/epja/i2013-13040-9.

[13] G.T. Koldste, et al., Relative proton and γ widths of astrophysically important states in ^{30}S studied in the β-delayed decay of ^{31}Ar, Phys. Rev. C 87 (2013) 055808, http://dx.doi.org/10.1103/PhysRevC.87.055808.

[14] H.O.U. Fynbo, et al., The $\beta 2p$ decay mechanism of ^{31}Ar, Nucl. Phys. A 677 (2000) 38, http://dx.doi.org/10.1016/S0375-9474(00)00248-7.

[15] I.S. Towner, J.C. Hardy, The evaluation of V_{ud} and its impact on the unitarity of the Cabibbo–Kobayashi–Maskawa quark-mixing matrix, Rep. Prog. Phys. 73 (2010) 046301.

[16] D. Wilkinson, B. Macefield, A parametrization of the phase space factor for allowed β-decay, Nucl. Phys. A 232 (1974) 58, http://dx.doi.org/10.1016/0375-9474(74)90645-9.

[17] L. Axelsson, et al., Beta decay of ^{31}Ar, Nucl. Phys. A 634 (4) (1998) 475, http://dx.doi.org/10.1016/S0375-9474(98)00172-9.

[18] B. Wildenthal, Empirical strengths of spin operators in nuclei, Prog. Part. Nucl. Phys. 11 (1984) 5, http://dx.doi.org/10.1016/0146-6410(84)90011-5.

[19] P. Hornshøj, et al., Beta-delayed proton emission from heavy nuclei: (ii). the calculation of spectral shapes and intensities in a compound-nucleus model, Nucl. Phys. A 187 (3) (1972) 609, http://dx.doi.org/10.1016/0375-9474(72)90685-9.